Origin of the Tunnel Anisotropic Magnetoresistance in $Ga_{1-x}Mn_xAs/ZnSe/Ga_{1-x}Mn_xAs$ Magnetic Tunnel Junctions of II-VI/III-V Heterostructures

H. Saito,* S. Yuasa, and K. Ando

Nanoelectronics Research Institute, National Institute of Advanced Industrial Science and Technology, Umezono 1-1-1, Central 2, Tsukuba, Ibaraki 305-8568, Japan

(Received 17 March 2005; published 17 August 2005)

We investigated spin-dependent transport in magnetic tunnel junctions made of III-V $Ga_{1-x}Mn_xAs$ electrodes and II-VI ZnSe tunnel barriers. The high tunnel magnetoresistance (TMR) ratio up to 100% we observed indicates high spin polarization at the barrier/electrodes interfaces. We found anisotropic tunneling conductance having a magnitude of 10% with respect to the direction of magnetization to linearly depend on the magnetic anisotropy energy of $Ga_{1-x}Mn_xAs$. This proves that the spin-orbit interactions in the valence band of $Ga_{1-x}Mn_xAs$ are responsible for the tunnel anisotropic magnetoresistance (TAMR) effect.

DOI: 10.1103/PhysRevLett.95.086604 PACS numbers: 72.25.Dc, 73.40.Gk, 75.50.Pp, 85.75.Dd

The spin-dependent transport phenomenon has been one of the major topics of research in the field of spintronics. Large tunnel magnetoresistance (TMR) in magnetic tunnel junctions (MTJs) [1–5] has enabled magnetoresistive random-access memories (MRAM) and the read heads of hard disk drives to be developed [6]. Most MTJs that have been studied up to now are based on 3*d*-ferromagnetic metal electrodes. Semiconductor-based MTJs are expected to become key components during the next step in multifunctional spintronic devices that will combine memory and logic functions [7] because several important material properties, such as carrier type (i.e., *n* or *p*) and carrier densities, can easily be controlled in semiconductor materials. However, the transport properties of semiconductor-based MTJs are not yet well understood.

p-type III-V $Ga_{1-x}Mn_xAs$ [8] is a prototype ferromagnetic semiconductor, and some results on the TMR effect in MTJs with $Ga_{1-x}Mn_xAs$ electrodes have been reported [9–13]. However, recent work has posed strong questions on interpretations of the reported TMR effect [14–16]. This controversial situation with semiconductor-based MTJs derives from large spin-orbit (SO) interaction in the valence band of $Ga_{1-x}Mn_xAs$. SO interaction in 3*d*-ferromagnetic metal is too weak to cause sizable modulations in the density of states at Fermi energy $D(E_F)$. Therefore, its effect on tunneling conductance G in metal-based MTJs can be neglected. However, SO interaction in $Ga_{1-x}Mn_xAs$ is expected to affect G [14] as well as magnetic properties such as magnetic anisotropy [17,18]. Indeed, recent observations of large anisotropic G with respect to the direction of magnetization in $Ga_{1-x}Mn_xAs$-based MTJs have been attributed to SO interactions [15,16], and a reexamination of previously reported TMR effects taking this tunnel anisotropic magnetoresistance (TAMR) effect into consideration is required. However, because the expected correspondence between large observed TAMR and magnetic anisotropy was not completely verified by Gould *et al.* [15] or Rüster *et al.* [16], the relations between TMR, TAMR, magnetic anisotropy, and SO interaction are still open to debate. It is crucial to clarify these issues before attempting to develop semiconductor-based spintronic devices.

In this study, we investigated spin-dependent transport phenomena in fully epitaxial $Ga_{1-x}Mn_xAs/ZnSe/Ga_{1-x}Mn_xAs$ MTJs. We adapted wide gap (2.8 eV) II-VI ZnSe for the barrier because it is a promising material for the *n*-type layer combined with GaAs [19,20]. The lattice constant of ZnSe (0.5669 nm) is very close to that of GaAs (0.5654 nm), and its optimum growth temperature is comparable to that of $Ga_{1-x}Mn_xAs$ ($\sim$250 °C). These properties make it possible to grow epitaxial n-ZnSe/p-$Ga_{1-x}Mn_xAs$ heterostructures [21,22]. Using these MTJs, we confirmed the intrinsic TMR effect with a high magnetoresistance (MR) ratio up to 100%. We also demonstrated there was a strong correlation between the TAMR effect, of the order of 10%, and the magnetic anisotropy energy of $Ga_{1-x}Mn_xAs$, indicating that the TAMR effect originates from SO interactions in the valence band of $Ga_{1-x}Mn_xAs$. Furthermore, our results posed further questions into the intrinsic nature of the large TAMR that has been reported.

The film for the MTJs was grown with molecular-beam epitaxy (MBE) using interconnected III-V and II-VI growth chambers. Before the growth, a surface oxide layer of epiready p^+-GaAs(001) (1×10^{19} cm^{-3}) substrate was removed by irradiating As_4 flux at 580 °C. A Be-doped (1×10^{19} cm^{-3}) 30 nm-thick GaAs buffer layer was first deposited at 560 °C. Then, a 50 nm-thick $Ga_{1-x}Mn_xAs$ ($x = 0.072$) bottom electrode, a 1 nm-thick ZnSe tunnel barrier layer, and a 50 nm-thick $Ga_{1-x}Mn_xAs$ ($x = 0.072$) top electrode were subsequently grown at 230 °C. The growth rates for $Ga_{1-x}Mn_xAs$ and ZnSe were 0.15 and 0.03 nm/s, respectively. The reflection high-energy electron diffraction (RHEED) images of the $Ga_{1-x}Mn_xAs$ layers exhibited a clear (1×2) reconstruction which is a typical pattern for high-quality $Ga_{1-x}Mn_xAs$ [8]. For the

ZnSe layer, the surface reconstruction was (2×1), indicating a Se-rich growth condition. A single layer of 50 nm-thick $Ga_{1-x}Mn_xAs$ ($x = 0.072$) with a hole concentration of 3×10^{20} cm^{-3} at 300 K was also grown under the same conditions as a reference. We prepared MTJs with a junction size of 10×10 μm^2 by using micro-fabrication techniques (e.g., photolithography and Ar ion milling). We did magnetization measurements with a superconducting quantum interference device (SQUID) magnetometer. The MR was measured using the dc four-probe method with a superconducting magnet equipped with a sample rotator. The direction of bias voltage V was defined with respect to the top $Ga_{1-x}Mn_xAs$ electrode.

Figure 1(a) plots the magnetization curves for the film at 5 K. Magnetic fields H were applied along [100] and [1$\bar{1}$0] directions. Double steps, which were caused by the different coercive forces between the two $Ga_{1-x}Mn_xAs$ electrodes, were more remarkable for $H\|[100]$. Corresponding MR curves for an MTJ at 2 K are plotted in Fig. 1(b). As was proven later, these MR results were due to the intrinsic TMR effect. The MR ratio is defined as $(R_{ap} - R_p)/R_p$, where R_{ap} and R_p are resistance when the magnetizations of the two electrodes are aligned antiparallel and parallel, respectively. Resistance-area product RA at a parallel alignment is 1.35×10^5 Ω μm^2 at 2 K. It should be noted that the MR ratio for $H\|[100]$ reached 100%. This value is among the highest ever reported for Fe/ZnSe/FeCo MTJs (~20%) [23,24] and comparable to those for $Ga_{1-x}Mn_xAs$-based MTJs with III-V semiconductor barriers [9–13]. A much smaller TMR ratio (41%) was observed for $H\|[1\bar{1}0]$, as expected from the corresponding magnetization curve. This was only because a particularly good antiparallel magnetization alignment was not achieved for $H\|[1\bar{1}0]$. Such different TMR ratios have been reported in $Ga_{1-x}Mn_xAs/AlAs/Ga_{1-x}Mn_xAs$ MTJs [10], which could well be explained by taking the in-plane magnetic anisotropy of $Ga_{1-x}Mn_xAs$ into account [10]. With increasing temperature, the TMR ratio rapidly decreased and almost disappeared above approximately 50 K. This is close to the Curie temperature, T_C, of the $Ga_{1-x}Mn_xAs$ single-layer reference sample of 60 K, and indicates that no significant reductions in T_C at the barrier/electrode interfaces occurred.

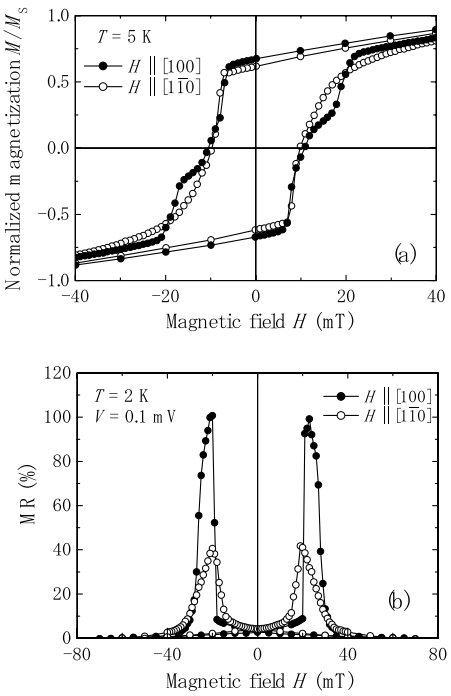

FIG. 1. (a) Magnetization curves at 5 K and (b) magnetoresistance curves at 2 K of $Ga_{1-x}Mn_xAs/ZnSe/Ga_{1-x}Mn_xAs$ MTJ. Solid and open circles correspond to data when magnetic fields were applied along [100] and [1$\bar{1}$0] directions, respectively. Magnetizations are normalized by saturation magnetization M_S.

Simmons' equation for current I versus bias-V characteristics for a parallel configuration yielded an effective barrier thickness of $t = 2.3$ nm and an effective barrier height of $\phi = 0.29$ eV, by assuming the effective mass of carriers m^* to be the free electron mass, m_0. Because m^*/m_0 in ZnSe should be less than unity, the obtained t and ϕ correspond to those lower and upper limits. The calculated t is still much thicker than the designed ZnSe barrier thickness (1 nm), suggesting depletion or interdiffusion at $ZnSe/Ga_{1-x}Mn_xAs$ interfaces. Nevertheless, the high TMR ratio that was observed of up to 100% indicates that high spin-polarized current could be tunneling across the effective tunnel barrier potential, including the depletion or interdiffusion regions.

To prove that the observed TMR was intrinsic, we investigated the effect of TAMR by measuring the angular dependence of G. The direction of the applied H is denoted by angles θ and φ with respect to the [001] and [100] crystallographic directions of the sample, respectively [Fig. 2(a)]. To rule out the influence of the TMR effect and to extract the TAMR signals from the MR curves, we did the measurements under magnetic fields sufficiently high to saturate the magnetizations of the two $Ga_{1-x}Mn_xAs$ layers along the H direction. Then, complete parallel alignment was maintained during the measurements. Figures 2(b) and 2(c) plot the normalized G of the MTJ at 2 K with 5 T as a function of θ and φ, respectively. Significant variations in G were observed. The conventional anisotropic magnetoresistance (AMR) effect of the electrodes cannot be used to explain the observed anisotropy in G because the resistance of the controlled sample without a ZnSe barrier (~10 Ω) was negligibly smaller than that of the present MTJ (~10^3 Ω). The G-θ curves exhibited maxima and minima when H was applied perpendicular ($\theta = 0°$ and $\pm 180°$) and parallel ($\theta = \pm 90°$) to the film plane, respectively. The TAMR ratio, defined as $(G_{[001]} - G_{[100]})/G_{[100]}$, was +10%, which is comparable to that of our previous experimental results for a CrTe/AlAs/$Ga_{1-x}Mn_xAs$ MTJ of +5.7% at 5 K [25]. The TAMR ratio decreased with increasing temperature. For

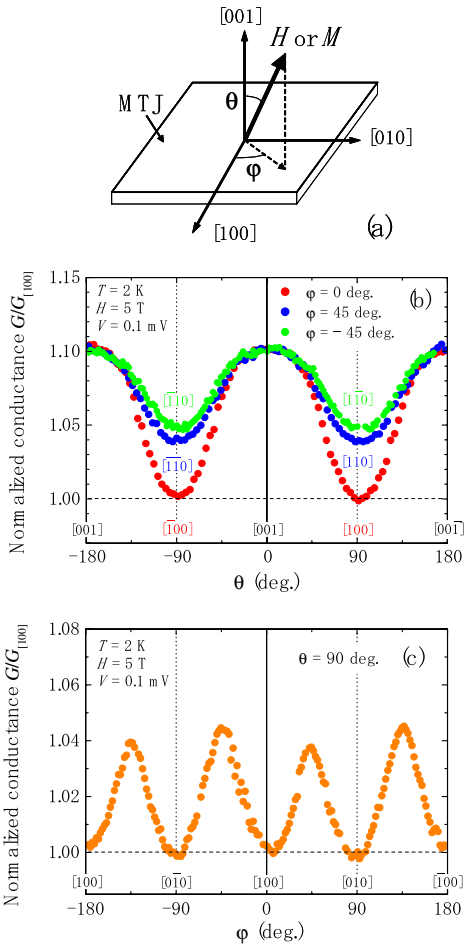

FIG. 2 (color online). (a) Coordinate system used for TAMR measurement. (b) and (c) Angular dependence of tunneling conductance of $Ga_{1-x}Mn_xAs/ZnSe/Ga_{1-x}Mn_xAs$ MTJ at 2 K with 5 T. Data are normalized by conductance $G_{[100]}$ where magnetic field was applied along [100] ($\theta = 90°$ and $\varphi = 0°$) direction.

example, the TAMR ratios were +9.8% and +8.5% at 10 K and 20 K, respectively. At $\theta = \pm 90°$, we found the relation $G_{[1\bar{1}0]}(\varphi = -45°) \geq G_{[110]}(\varphi = 45°) > G_{[001]}(\varphi = 0°)$. No differences in G were identified in the G-φ curve within experimental error when H was applied along the in-plane cubic easy magnetization axes of $\langle 100 \rangle$ ($\varphi = 0°$, $\pm 90°$, and $\pm 180°$). This indicates that the observed TMR effect in Fig. 1(b) is free of the TAMR effect. The shape of the angular dependence of G is independent of H up to 9 T and of bias V up to 95 mV. We should point out that the directions in which the maximum and minimum in G were observed correspond to the perpendicular uniaxial hard and in-plane cubic easy magnetization axes of $Ga_{1-x}Mn_xAs$ film on the GaAs substrate [26,27]. This implies that the TAMR has a correlation with the magnetic anisotropy of $Ga_{1-x}Mn_xAs$.

We estimated the magnetic anisotropy energy F_A of $Ga_{1-x}Mn_xAs$ film with ferromagnetic resonance (FMR) measurement for quantitative analysis. The FMR measurement was conducted at 4.5 K at 9.04 GHz under H up to 1.2 T. We used the $Ga_{1-x}Mn_xAs$ single reference layer sample. When H was applied along the [001], [1$\bar{1}$0], [110], and [100] directions, the observed FMR fields H_R we obtained were 0.61, 0.38, 0.28, and 0.088 T, respectively. F_A was estimated as follows when the $M \| H$, F_A of $Ga_{1-x}Mn_xAs$ film is described by the following equation [27,28],

$$F_A = F + MH = -2\pi M^2 \sin^2\theta - K_{2\perp}\cos^2\theta - \frac{1}{2}K_{4\perp}\cos^4\theta + \frac{1}{2}K_{4\|}\frac{1}{4}(3 + \cos 4\varphi)\sin^4\theta - K_{2\|}\sin^2\theta \sin^2\left(\varphi - \frac{\pi}{4}\right), \quad (1)$$

where F is the total magnetic free energy, and $K_{2\perp}$ and $K_{4\perp}$ are the respective perpendicular uniaxial and cubic anisotropy constants. The $K_{2\|}$ and $K_{4\|}$ represent in-plane uniaxial and cubic anisotropy, respectively. From the observed H_R and equations for the resonance conditions obtained from Eq. (1) [27], anisotropy fields $2K_{2\perp}/M$, $2K_{2\|}/M$, and $2K_{4\|}/M$ were obtained as -0.21, -0.045, and 0.15 T, respectively, which are close to the reported values [27]. The value of F_A in specific directions can be obtained by substituting these constants in Eq. (1). The value of $K_{4\|}$ was used for $K_{4\perp}$ since it is difficult to reliably estimate $K_{4\perp}$ due to the large contribution from $K_{2\perp}$ [27]. The relation between F_A and G is plotted in Fig. 3. An almost linear relation with a slope of $\sim 6\%/(\mathrm{kJ\,m^{-3}})$ between G and F_A can clearly be identified. This indicates that the TAMR effect and magnetic anisotropy have the same origin, i.e., the anisotropic $D(E_F)$ of $Ga_{1-x}Mn_xAs$ due to SO interactions in the valence band of $Ga_{1-x}Mn_xAs$.

It should be noted that the present results for TAMR significantly differ from the previous theoretical [14] and

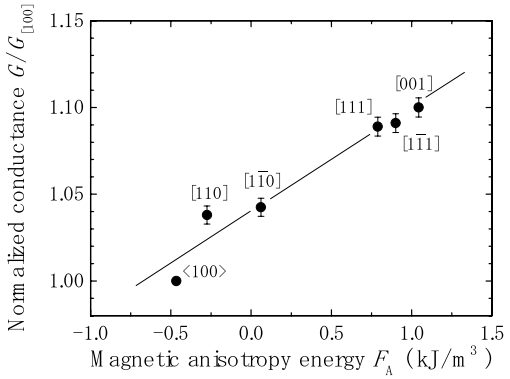

FIG. 3. Normalized tunneling conductance of $Ga_{1-x}Mn_xAs/ZnSe/Ga_{1-x}Mn_xAs$ MTJ vs magnetic anisotropy energy of $Ga_{1-x}Mn_xAs$ in specific directions. Tunneling conductance was measured at 2 K and 0.1 mV with 5 T. Magnetic anisotropy energies were obtained by ferromagnetic resonance measurements of single-layer $Ga_{1-x}Mn_xAs$ sample at 4.5 K.

experimental results [15,16]. The sign for TAMR was obtained from the calculated valence band of $Ga_{1-x}Mn_xAs$ based on mean-field and virtual-crystal (MF-VC) approximation [14], which has been widely used to explain the magnetic properties of $Ga_{1-x}Mn_xAs$ [17,18]. The predicted sign for TAMR was negative, which is inconsistent with observed TAMR data with a positive sign. This implies that the valence band structure of $Ga_{1-x}Mn_xAs$ near E_F obtained from MF-VC approximation is not realistic. We therefore need to reexamine the valence band structure of $Ga_{1-x}Mn_xAs$. Experimental results [15,16] revealed a very large TAMR ratio up to 150 000% in $Ga_{1-x}Mn_xAs$-based MTJs when the magnetizations were switched between the in-plane easy axes of [100] and [010] while no TAMR was detected in our MTJ, as is shown in Fig. 2(c). Additional magnetic anisotropy, whose origin is not verified, was necessary to explain the TAMR behavior by introducing a uniaxial strain along the [010] axis [15,16]. This strongly suggests that $Ga_{1-x}Mn_xAs$ electrodes lost their characteristic magnetic anisotropy due to significant depletion near the barrier [16].

In summary, we investigated spin-dependent transport in fully epitaxial $Ga_{1-x}Mn_xAs/ZnSe/Ga_{1-x}Mn_xAs$ consisting of II-VI/III-V heterostructures. An intrinsic TMR effect up to 100% was observed at 2 K, indicating high spin polarization at the barrier/electrode interfaces. This is an important first step to achieving a spin-bipolar device [29,30] by using n-ZnSe/p-$Ga_{1-x}Mn_xAs$ heterostructures. We also demonstrated essential features of TAMR in $Ga_{1-x}Mn_xAs$-based MTJs. We found a linear relation between F_A of $Ga_{1-x}Mn_xAs$ and G of the MTJ with respect to the direction of magnetization. This experimentally proved that the origin of TAMR is the anisotropic $D(E_F)$ of $Ga_{1-x}Mn_xAs$ with respect to magnetization due to its strong SO interactions in the valence band.

The authors are grateful to Dr. Taro Nagahama (AIST), Professor Yoshishige Suzuki (Osaka University), and Dr. Eichi Tamura for their valuable discussions. They also wish to thank Dr. Yuko Yokoyama and Mrs. Mie Yamamoto (AIST) for helping prepare the samples, and Mr. Satoshi Yakata, Professor Yasuo Ando, and Professor Terunobu Miyazaki (Tohoku University) for doing the FMR measurements.

*Corresponding author.
Email: h-saitoh@aist.go.jp

[1] T. Miyazaki and N. Tezuka, J. Magn. Magn. Mater. **139**, L231 (1995).
[2] J. S. Moodera, L. R. Kinder, T. M. Wong, and R. Meservey, Phys. Rev. Lett. **74**, 3273 (1995).
[3] S. Yuasa, T. Nagahama, A. Fukushima, Y. Suzuki, and K. Ando, Nat. Mater. **3**, 868 (2004).
[4] S. S. P. Parkin, C. Kaiser, A. Panchula, P. M. Rice, B. Hughes, M. Samant, and S. H. Yang, Nat. Mater. **3**, 862 (2004).
[5] D. D. Djayaprawira, K. Tsunekawa, M. Nagai, H. Maehara, S. Yamagata, N. Watanabe, S. Yuasa, Y. Suzuki, and K. Ando, Appl. Phys. Lett. **86**, 092502 (2005).
[6] S. A. Wolf, D. D. Awschalom, R. A. Buhrman, J. M. Daughton, S. von Molnár, M. L. Roukes, A. Y. Chtchelkanova, and D. M. Treger, Science **294**, 1488 (2001).
[7] I. Žutić, J. Fabian, and S. Das Sarma, Rev. Mod. Phys. **76**, 323 (2004).
[8] H. Ohno, A. Shen, F. Matsukura, A. Oiwa, A. Endo, S. Katsumoto, and Y. Iye, Appl. Phys. Lett. **69**, 363 (1996).
[9] M. Tanaka and Y. Higo, Phys. Rev. Lett. **87**, 026602 (2001).
[10] Y. Higo, H. Shimizu, and M. Tanaka, J. Appl. Phys. **89**, 6745 (2001).
[11] R. Mattana, J.-M. George, H. Jaffrès, F. Nguyen Van Dau, A. Fert, B. Lépine, A. Guivarc'h, and G. Jézéquel, Phys. Rev. Lett. **90**, 166601 (2003).
[12] S. H. Chun, S. J. Potashnik, K. C. Ku, P. Schiffer, and N. Samarth, Phys. Rev. B **66**, 100408(R) (2002).
[13] D. Chiba, F. Matsukura, and H. Ohno, Physica E (Amsterdam) **21**, 966 (2004).
[14] L. Brey, C. Tejedor, and J. Fernández-Rossier, Appl. Phys. Lett. **85**, 1996 (2004).
[15] C. Gould, C. Rüster, T. Jungwirth, E. Girgis, G. M. Schott, R. Giraud, K. Brunner, G. Schmidt, and L. W. Molenkamp, Phys. Rev. Lett. **93**, 117203 (2004).
[16] C. Rüster, C. Gould, T. Jungwirth, J. Sinova, G. M. Schott, R. Giraud, K. Brunner, G. Schmidt, and L. W. Molenkamp, Phys. Rev. Lett. **94**, 027203 (2005).
[17] M. Abolfath, T. Jungwirth, J. Brum, and A. H. MacDonald, Phys. Rev. B **63**, 054418 (2001).
[18] T. Dietl, H. Ohno, and F. Matsukura, Phys. Rev. B **63**, 195205 (2001).
[19] A. S. Glaeser, J. L. Merz, R. E. Nahory, and M. C. Tamargo, Appl. Phys. Lett. **60**, 1345 (1992).
[20] I. Malajovich, J. J. Berry, N. Samarth, and D. D. Awschalom, Nature (London) **411**, 770 (2001).
[21] S. H. Chun, K. C. Ku, S. J. Potashnik, P. Schiffer, and N. Samarth, J. Vac. Sci. Technol. B **20**, 1266 (2002).
[22] N. Samarth, S. H. Chun, K. C. Ku, S. J. Potashnik, and P. Schiffer, Solid State Commun. **127**, 173 (2003).
[23] F. Gustavsson, J.-M. George, V. H. Etgens, and M. Eddrief, Phys. Rev. B **64**, 184422 (2001).
[24] X. Jiang, A. F. Panchula, and S. S. P. Parkin, Appl. Phys. Lett. **83**, 5244 (2003).
[25] H. Saito, S. Yuasa, and K. Ando, J. Appl. Phys. **97**, 10D305 (2005).
[26] H. Ohno, F. Matsukura, A. Shen, Y. Sugawara, A. Oiwa, A. Endo, S. Katsumoto, and Y. Iye, in *Proceedings of the 23rd International Conference on Physics of Semiconductors, Berlin 1996*, edited by M. Scheffler and R. Zimmermann (World Scientific, Singapore, 1996), p. 405.
[27] X. Liu, Y. Sasaki, and J. K. Furdyna, Phys. Rev. B **67**, 205204 (2003).
[28] M. Farle, Rep. Prog. Phys. **61**, 755 (1998).
[29] M. E. Flatté, Z. G. Yu, E. Johnston-Halperin, and D. D. Awschalom, Appl. Phys. Lett. **82**, 4740 (2003).
[30] J. Fabian, I. Žutić, and S. Das Sarma, Appl. Phys. Lett. **84**, 85 (2004).